

INCLUSIVE ANGULAR DISTRIBUTION OF α AND Li FRAGMENTS PRODUCED
IN THE Fe-C AND Fe-Pb COLLISIONS AT 1.88 GeV/u*

C. O. Kim and S. N. Kim
Department of Physics, Korea University, Seoul 132, Korea
and

I. K. Chae and D. H. Kim
Department of Physics, Sookmyung Women's University
Seoul 140, Korea

ABSTRACT

The LS (laboratory system) emission angles θ for 2188 α and 298 Li fragments, produced inclusively in relativistic Fe-C and Fe-Pb collisions, have been measured in reference to incident Fe-ion beam tracks nearby in nuclear emulsion. An empirical differential frequency formula,

$$dN(\cot \theta) = \exp(a + b \cot \theta) d(\cot \theta) \quad (1)$$

is obtained with the constant $b \cong -0.026$ at 1.88 GeV/u, which seems to be independent on the kinds of target nucleus as well as on the kinds of projectile fragments. Equation (1) supports the conventional Kaplon's formula,¹ which has been a convenient tool for estimating the unknown primary energy of cosmic-ray primaries;

$$\langle \theta^2 \rangle^{\frac{1}{2}} = \zeta/u \delta_p, \quad (2)$$

with $\zeta = -0.056$, where $u \delta_p$ is the primary energy in GeV/nucleon. Also, the significance of Eq. (1) is discussed.

1. Introduction. When nuclear interactions produced by high-energy singly-charged hadrons in nuclear emulsion ("stars") are observed in the LS, very slow fragments of the constituent nuclei (Ag, Br, C, N, O, H) of nuclear emulsion can be readily distinguished from relativistic shower particles. Nevertheless, it is usually difficult to identify these nonrelativistic fragments, mainly due to their high ionization and short track lengths. Now, owing to recent development in accelerating heavy ions, the "heavy evaporation fragments" in the projectile rest system (ALS; anti-laboratory system) can be observed as 'relativistic particles' in the LS. Particularly, the relativistic α and Li fragments are identified with ease in nuclear emulsion just by simple inspection through an optical microscope, since the former have about four times the grain density of minimum-ionizing tracks, and the latter about nine times. This very technique of identifying α fragments has been used by some recent angular measurements.²

* Research supported partly by Korea Science and Engineering Foundation (KOSEF) (1984-87).

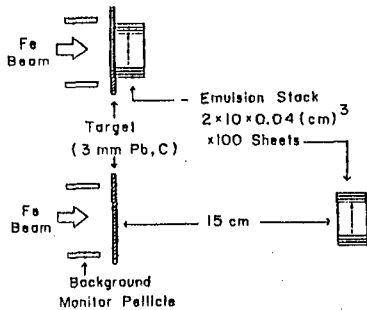


Fig. 1. Experimental Setup.

pellicles were exposed 'horizontally' to the Fe-ion beam with a track density of about 5×10^3 ions/cm².

Because of large distortion present up to $\sim 500 \mu\text{m}$ from the entrance edges of pellicles, α and Li fragments were picked usually at $\sim 500 \mu\text{m}$ from the edges, and angular measurements were typically performed at $\sim 1 \text{ mm}$ downstream from the entrance edges. Special attention was given not to miss such α and Li fragments as were produced with large θ . In order to avoid the effect due to the distortion inherent in the processed emulsion plate, the LS emission angles θ were measured by use of the reference-track method,³ i. e., always in reference to nearby Fe-ion beam tracks, which had the angular deviation of 2.3 ± 0.3 and 3.7 ± 0.3 mrad., respectively, for the pellicles behind the carbon and lead targets at the site of angular measurements.

3. Experimental Results. As shown in Fig. 2, the differential frequency $dN(\theta)$ versus θ (vacant circles for Fe-C collisions and filled circles for Fe-Pb collisions) resemble closely those of Ref. 2. The two plots in the above for each of S-stacks and L-stacks shown separately and the combined data are shown in the lowest in Fig. 2. There seem to be tendencies of more population of α fragments in the extreme angular regions of $\theta > 10^\circ$ and of $\theta \leq 1^\circ$ for Fe-C collisions than for Fe-Pb collisions. The results of fitting the angular data of $\theta \leq 3^\circ$ with the Gaussian regression function (χ^2/DF , 10 - 30) and those of $\theta \leq 5^\circ$ with the exponential regression function (χ^2/DF , 1 - 2) are also indicated as the curves and equations in the figure.

The root-mean-square angles of fragments (Li fragments) $(\langle \theta^2 \rangle)^{1/2}$, for $\theta < 5^\circ$, as advocated in Ref. 1, are 0.037 ± 0.02 and 0.038 ± 0.01 (0.032 ± 0.02 and 0.035 ± 0.01), respectively, for Fe-C and Fe-Pb collisions, which correspond to $\bar{\lambda} = 0.057$ and 0.067 (0.056 and 0.062) in Eq. (2).

But, we find it most reasonable and revealing to plot the differential frequency $dN(\cot \theta)$ versus, as shown in Fig. 3 (a) for Fe-C collisions and (b) for the Fe-Pb collisions. In the figures the filled circles represent the angular data from 2188 α fragments, and the vacant circles those from 298 Li

2. Experimental Setup and Method. The specific arrangements of the experiment to the Fe-ion beam of 1.88 GeV/u at the Lawrence Berkeley Bevalac are illustrated in Fig. 1. The 3 mm-thick target was made of either carbon or lead. The detector of fragments and incident Fe ions is an emulsion stack (made of 100 Fuji ET7B pellicles of sheet size, $2 \times 10 \times 0.04 \text{ cm}^3$) and is either placed just behind the target plate ("S-stacks") or 15 cm away from the back of the target plate ("L-stacks") in downstream. The shorter edges of

fragments. Since no statistically significant differences between the angular data of S-stacks and those of L-stacks were detected, only the combined data are shown in the figure. For the least-square fit, we used the regression function,

$$\frac{dN(\cot \theta)}{\exp(a + b \cot \theta) d(\cot \theta)} \quad (1)$$

with reasonable fits to most of the angular data, as seen from the best fitted values of a and b and χ^2/DF , separately, for Fe-C and Fe-Pb collisions in Table I. In Figs. 3, the straight lines in the figures and the dotted lines in the inserts show the best-fitted curves. For the interval of $\cot \theta = 0-20$, the amplified version of $dN(\cot \theta)$ versus $d(\cot \theta)$ with one-tenth the interval in the main figures are shown as the inserts, sharp fall-offs of $dN(\cot \theta)$ for $\cot \theta \leq 4$ can be seen. But those portions of α and Li fragments, with extremely small and large θ , which deviates appreciably from the general trends represented by Eq. (1) constitute only several percents.

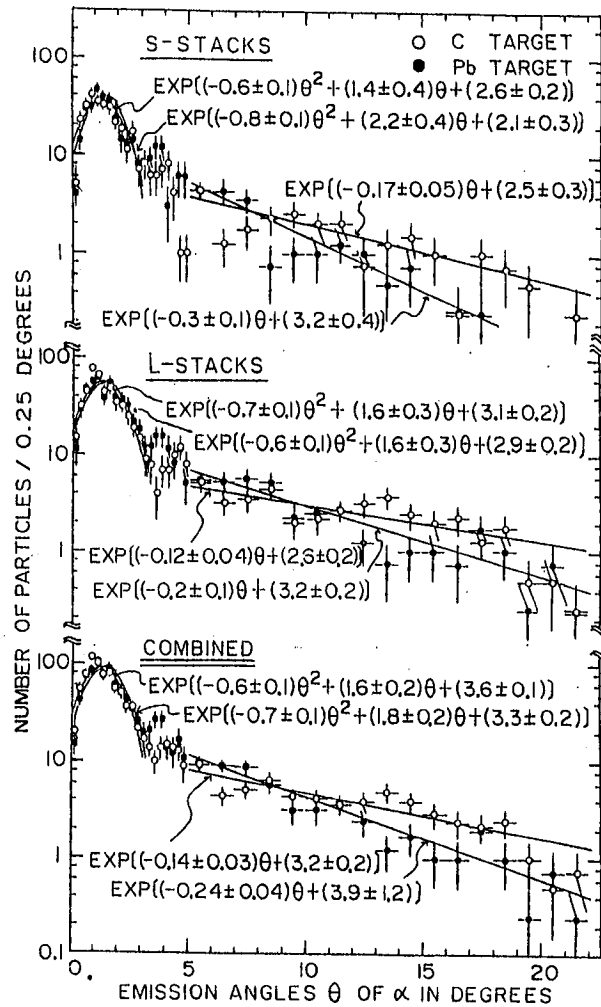


Fig. 2

Table I. The fitted values of a and b of Eq. (1) from the angular data of α fragments (and of Li fragments inside the brackets).

Target	# of α fragments = # from S-stacks + # from L-stacks	a	b	χ^2/DF
Carbon	1103 = 408 + 695 (138 = 35 + 103)	6.3 ± 0.05 (4.4 ± 0.1)	0.0248 ± 0.0009 (0.029 ± 0.003)	21/9 (6/5)
	1085 = 408 + 677 (160 = 62 + 98)	6.3 ± 0.04 (4.4 ± 0.1)	0.0265 ± 0.0009 (0.030 ± 0.003)	27/10 (11/5)

4. Discussion and Conclusion.
From the Lorentz transformation of $\cot \theta$ from the LS to the ALS,

$$\cot \theta = \frac{M_F \bar{\gamma}_p \bar{\gamma} (\bar{\beta} \cos \bar{\theta} + \beta_p)}{M_F \bar{\gamma} \bar{\beta} \sin \bar{\theta}} \approx \bar{\gamma}_p \beta_p / (\bar{\beta} \sin \bar{\theta}), \quad (3)$$

where we used the fact that

$$\bar{\beta} \cos \bar{\theta} \ll \beta_p \quad (4)$$

from the observation of D. E. Greiner et al.⁴ as well as our experience with the heavy evaporation prongs produced in high-energy jets in nuclear emulsion. Thus, we obtain the target-independent formula,

$$dN(1/\bar{\beta} \sin \bar{\theta}) \approx (\kappa/b) \times \exp(a + \kappa/\bar{\beta} \sin \bar{\theta}) \times d(1/\bar{\beta} \sin \bar{\theta}), \quad (5)$$

with a Lorentz-invariant constant,

$$\kappa = \bar{\gamma}_p \beta_p b. \quad (6)$$

In fact, Eq. (1) along with Eq. (6) is in accord with the Kaplon's formula, Eq. (2), by finding the median angle through integration of Eq. (1), as

$$\cot \theta_{\frac{1}{2}} = \ln 2/|b| = (\ln 2) (\bar{\gamma}_p \beta_p)/|\kappa|. \quad (7)$$

This method gives the value of $\zeta = 0.06 - 0.07$ in Eq. (2).

REFERENCES

- 1M. F. Kaplon et al., Phys. Rev. 85, 295 (1952).
- 2H. H. Heckman et al., Phys. Rev. C 17, 1735 (1978); K. B. Balla et al., Nucl. Phys. A367, 446 (1981); M. M. Aggarwal et al., Phys. Rev. C 27, 640 (1983); G. M. Chernov et al., Nucl. Phys. A412, 534 (1984).
- 3C. O. Kim, Phys. Rev. D 31, 513 (1985).
- 4D. E. Greiner et al., Phys. Rev. Lett. 35, 152 (1975).

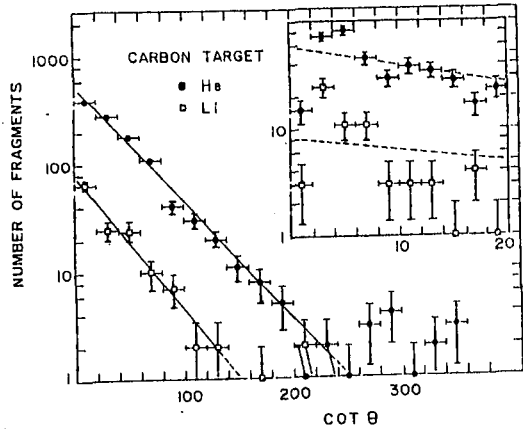


Fig. 3 (a)

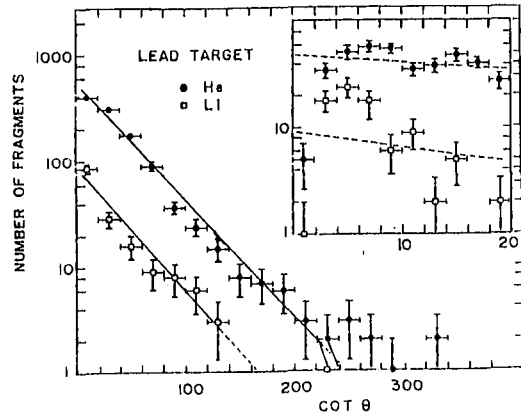


Fig. 3 (b)